

Development of Quasi-Monoenergetic Neutron Source Using the $1\text{H}(13\text{C},n)$ Reaction

Watanabe, Yukinobu

Department of Advanced Energy Engineering Science, Interdisciplinary Graduate School of Engineering Sciences, Kyushu University

Matsuoka, Yasuaki

Kyushu Electric Power Corporation | Department of Advanced Energy Engineering Science, Interdisciplinary Graduate School of Engineering Sciences, Kyushu University

Nakamura, Hiroshi

Nomura Research Institute | Department of Advanced Energy Engineering Science, Interdisciplinary Graduate School of Engineering Sciences, Kyushu University

Nakashima, Hideki

Department of Advanced Energy Engineering Science, Interdisciplinary Graduate School of Engineering Sciences, Kyushu University

他

<https://doi.org/10.15017/16640>

出版情報：九州大学大学院総合理工学報告. 23 (3), pp.285-290, 2001-12. 九州大学大学院総合理工学府

バージョン：

権利関係：

Development of Quasi-Monoenergetic Neutron Source Using the ${}^1\text{H}({}^{13}\text{C},n)$ Reaction

Yukinobu WATANABE*^{1,†}, Yasuaki MATSUOKA*², Hiroshi NAKAMURA*³,
Hideki NAKASHIMA*¹ Nobuo IKEDA*⁴ and Kenshi SAGARA*⁵

[†]E-mail of corresponding author: *watanabe@aees.kyushu-u.ac.jp*

(Received October 31, 2001)

We have developed a new type of monoenergetic neutron source at the Kyushu University Tandem Laboratory using the inverse (p,n) reaction kinematics. The ${}^1\text{H}({}^{13}\text{C},n)$ reaction was chosen as a promising candidate. A major part of the neutron source consists of a hydrogen gas target having an entrance window made of 3 μm -thick tantalum foil and a 0.2 mm-thick tantalum disk as the beam stopper. An experiment for the feasibility test was performed using 56.0 and 59.3 MeV ${}^{13}\text{C}^{6+}$ beams. The preliminary result showed that the ${}^1\text{H}({}^{13}\text{C},n)$ reaction can produce the kinematically-collimated monoenergetic neutrons in the MeV region.

Key words : *Accelerator-driven neutron source, Quasi-monoenergetic neutron, MeV-region, Inverse kinematics, ${}^1\text{H}({}^{13}\text{C},n)$, Gas target, NE213 detector*

1. Introduction

There are various types of accelerator-driven neutron sources that are widely utilized in basic science and applications. In the energy region covered by tandem Van de Graaf accelerators, light-ion induced reactions on light element targets, such as the $\text{D}(d,n)$ and $\text{T}(d,n)$ reactions, are the most commonly used as the nuclear reactions to produce monoenergetic neutrons. However, these reactions cannot produce monoenergetic neutrons in the energy region between 8 and 14 MeV, because of the breakup of the projectile and/or the target nucleus. Therefore, only few neutron cross section data are now available in this "gap" energy region, whereas the data in this energy region are required in several applications, e.g., development of D-T fusion reactors.

Recently, new types of monoenergetic neutron sources with heavy ion (HI) beams have been proposed as one of the candidates to fill in the "gap" region and the feasibility has so far been

investigated.¹⁻³⁾ Among these studies about the ${}^1\text{H}(\text{HI},n)$ reaction, a neutron source with the ${}^1\text{H}({}^{11}\text{B},n)$ reaction was practically used for measurements of activation cross sections in the 9 to 13 MeV region⁴⁾ and its usefulness had been demonstrated.

Characteristic features and advantages of the ${}^1\text{H}(\text{HI},n)$ neutron source are summarized as follows:

- 1) Neutrons are emitted at angles smaller than θ_{max} defined by two-body kinematics in an endothermic reaction, that is, "kinematically collimated" neutrons are produced. This situation is illustrated schematically in Fig. 1. By this collimation, the shielding design of neutron facilities is expected to become easier.
- 2) The ${}^1\text{H}(\text{HI},n)$ cross section at 0° in the laboratory system is enhanced strongly by the compression into the forward cone, which is expected to lead to large neutron yield at 0° .
- 3) Emitted neutrons have two energies as shown in Fig. 1. However, the yield of neutrons with lower energy is considerably smaller than those with higher energy under most experimental conditions.
- 4) Backgrounds of neutrons and γ rays from the beam stopper can be reduced, because heavy

*1 Department of Advanced Energy Engineering Science

*2 Graduate student, Department of Advanced Energy Engineering Science, (Present affiliation: Kyushu Electric Power Corporation)

*3 Graduate student, Department of Advanced Energy Engineering Science, (Present affiliation: Nomura Research Institute)

*4 Department of Applied Quantum Physics and Nuclear Engineering, Faculty of Engineering

*5 Department of Physics, Faculty of Science

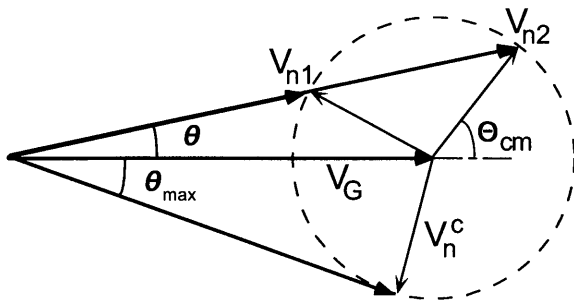


Fig. 1 Schematic diagram of two-body kinematics for the ${}^1\text{H}(\text{HI},n)$ reaction under the condition $V_G > V_n^c$, where V_G denotes the velocity of the center of mass(CM), and V_n^c that of the produced neutron in the CM system. θ_{max} is the maximum angle of neutron production in the laboratory system.

projectiles have higher Coulomb barrier than protons and deuterons.

At the Kyushu University Tandem Laboratory(KUTL), we have started to develop a monoenergetic neutron source in the "gap" region by using the ${}^1\text{H}(\text{HI},n)$ reaction. The ${}^1\text{H}({}^{13}\text{C},n)$ reaction was chosen as a candidate suitable for KUTL from consideration about the performance of accelerator, and its feasibility test has been performed in the present work.

2. Design of neutron source and its simulation

The neutron source developed in the present work consists of a hydrogen gas target which is shown schematically in Fig. 2. The gas cell is made of 0.5 mm-thick stainless steel and has the effective size of 30 mm long and 30 mm in diameter. The entrance window is made of tantalum foil of 3 μm in thickness and 12 mm in diameter on a cylinder shape frame of curvature 6 mm. A 0.2 mm-thick tantalum disk is used as the beam stopper so that associated background neutrons and γ rays may be reduced as much as possible by using high Z materials. Escape of the electrons produced by beam bombardment on the entrance window is suppressed by permanent magnets.

In the design of the neutron source, we have estimated neutron yields at 0° using a modified version of the simulation code developed for the ${}^1\text{H}({}^{11}\text{B},n)$ neutron source.⁹⁾ Cross sections of the ${}^1\text{H}({}^{13}\text{C},n)$ reaction as a function of incident energy are necessary for the estimation. However, there is no available experimental data. Therefore, those

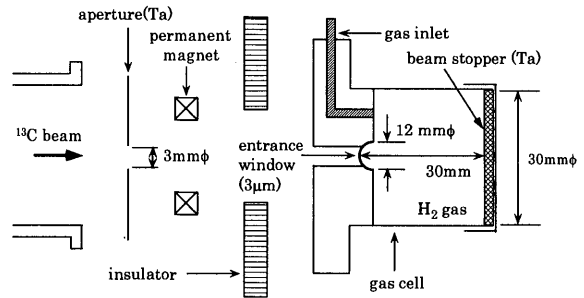


Fig. 2 Schematic drawing of the hydrogen gas target.

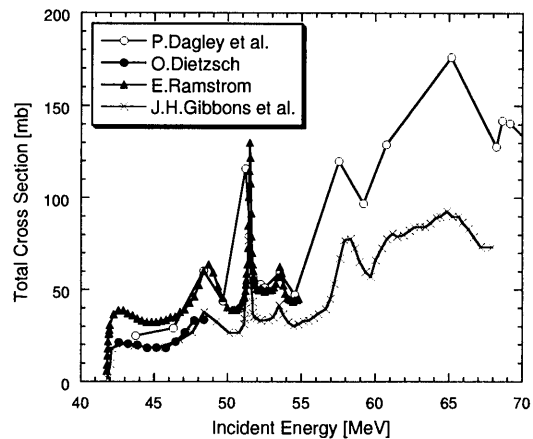


Fig. 3 Total cross sections of the ${}^1\text{H}({}^{13}\text{C},n)$ reaction derived from experimental total cross sections of the ${}^{13}\text{C}(p,n)$ reaction.

cross sections are derived from the ${}^{13}\text{C}(p,n)$ cross sections in terms of the inverse kinematics. Available experimental data⁵⁻⁸⁾ of the total ${}^{13}\text{C}(p,n)$ cross sections are plotted in Fig. 3. The data of Dagley et al.⁶⁾ who measured the angular distributions of emitted neutrons were employed in the simulation because the ${}^{13}\text{C}(p,n)$ cross sections at 0° and 180° in the CM system are necessary for estimation of the neutron yields of the ${}^1\text{H}({}^{13}\text{C},n)$ reaction at 0° . The obtained differential ${}^1\text{H}({}^{13}\text{C},n)$ cross sections in the laboratory system are also given in Fig. 4; the upper and lower panels correspond to high energy ("primary") component and low energy ("satellite") component of neutrons generated by the two-body kinematics illustrated in Fig. 1, respectively.

Figure 5 shows an example of the estimated neutron yield at an incident ${}^{13}\text{C}$ energy of 58.2 MeV. The gas pressure was chosen to be 1 atm. The incident energy was adjusted to become a resonance energy of about 51.5 MeV shown in Fig. 3 at the center of the gas cell. One can see two peaks corre-

sponding to two neutron components. It is found that the yield of "primary" neutrons having the energy of about 7 MeV is much larger than that of "satellite" neutrons having the energy of about 1 MeV. The difference in the yields can be easily explained from that in the cross sections shown in Fig. 4.

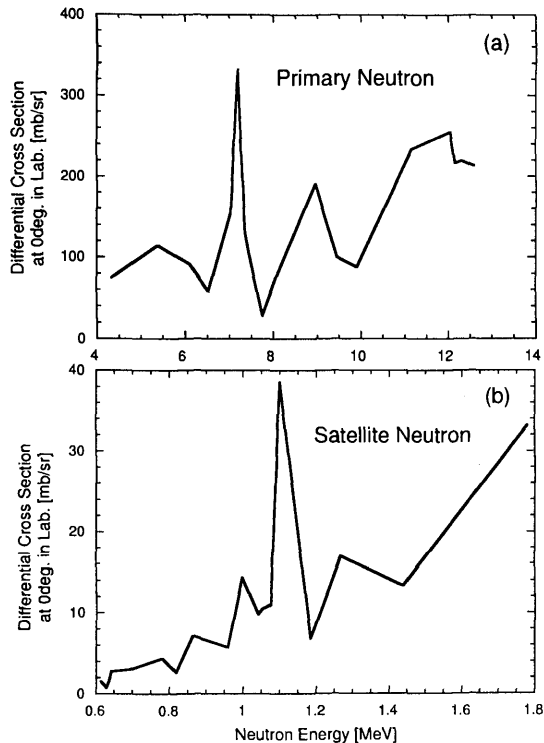


Fig. 4 Differential $^1\text{H}(^{13}\text{C},n)$ cross sections in the laboratory system. Neutrons generated by the two-body kinematics have two components as shown in Fig. 1: (a) high energy ("primary") component and (b) low energy ("satellite") component.

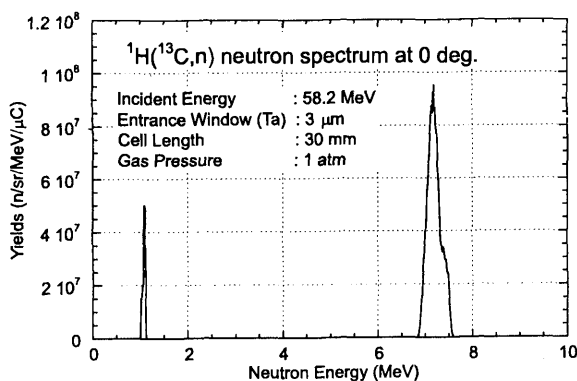


Fig. 5 Calculated spectrum of neutrons produced by the $^1\text{H}(^{13}\text{C},n)$ reaction at 58.2 MeV in the 0° direction.

3. Experiment

An experiment to test the feasibility of the neutron source was carried out using 56.0 MeV and 59.3 MeV $^{13}\text{C}^{6+}$ beams at KUTL. These incident energies were determined by the above-mentioned simulation so that the energies of primary neutrons generated at 0° were 6.2 and 7.2 MeV, respectively. The average beam current was about 10 to 40 nA. The pressure of hydrogen gas in the gas cell was 2 atm. Emitted neutrons were detected using a 7.6-cm diameter and 15.2-cm thick NE213 scintillator coupled to a photomultiplier tube (PMT: Hamamatsu R1821-01) placed 2 m downstream from the center of the hydrogen gas target. In the following signal processing,^{10,11)} background events due to gamma-rays were eliminated by using a conventional pulse shape discrimination (PSD) method. Neutron yields were measured at angles between 0° and 35° in step of 5° for 59.3 MeV, and only 0° for 56.0 MeV. An active radiator proton recoil telescope (ARPRT) developed by our group¹²⁾ was also used for the measurement at 0° to check the absolute yield. The ARPRT was located 20 cm far from the center of the gas cell. To estimate background neutrons generated from the entrance window and beam stopper in the gas cell, those scattered by the surrounding walls and floor, the following background runs were carried out using a $20 \times 20 \times 40 \text{ cm}^3$ shadow bar made of iron: (1) gas-in and with shadow bar, (2) gas-out and with shadow bar (3) gas-out and without shadow bar.

An additional experiment for the well-known $\text{D}(d,n)$ reaction was also performed using the same gas target for comparisons with the result of the $^1\text{H}(^{13}\text{C},n)$ reaction. The D_2 gas filled in the gas cell had the pressure of 2 atm. The incident deuteron energy of 4.3 MeV was chosen so as to give the same neutron energy of 7.2 MeV as the $^1\text{H}(^{13}\text{C},n)$ reaction. It should be noted that a 7.2 MeV neutron generated by the $\text{D}(d,n)$ reaction is monoenergetic because the incident deuteron energy is lower than the threshold energy of breakup reactions, *e.g.*, the $\text{D}(d,np)$ reaction. Neutron yields from the $\text{D}(d,n)$ reaction were measured at angles between 0° and 70° in step of 10° .

4. Experimental results and discussion

A two-dimensional plot of output signals from the PMT dynode and the PSD circuit is shown for a foreground (FG) run with gas-in and without shadow bar in Fig. 6. Neutron events are sep-

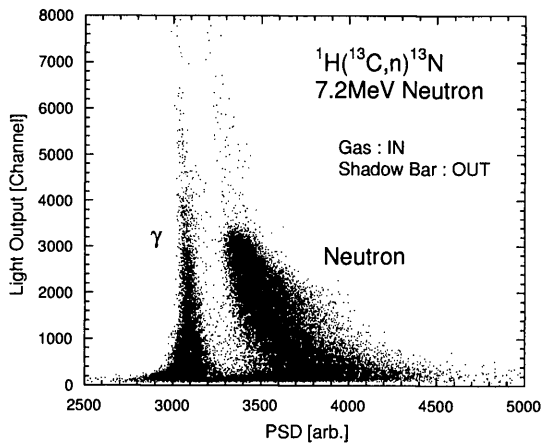


Fig. 6 Two-dimensional plot of pulse height distributions from the PMT dynode and the PSD circuit.

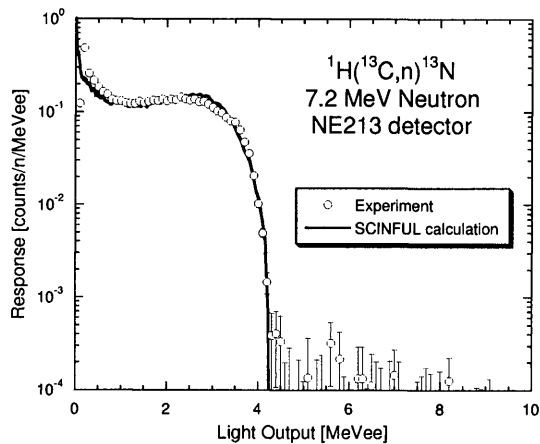


Fig. 7 Measured and calculated NE213 response functions for the neutron measurement at 0° for the ${}^1\text{H}({}^{13}\text{C},n){}^{13}\text{N}$ reaction at 59.3 MeV.

arated well from background gamma-rays events. After the separation of the gamma-ray background events, a pulse height spectrum of neutrons coming directly from the neutron source were obtained using the following relation, $FG - BG(1) - BG(2) + BG(3)$, where $BG(i)$ ($i=1,2,3$) correspond to the above-mentioned three background events. In Fig. 7, the resultant pulse height spectrum at 0° is compared with the calculated NE213 response function with the SCINFUL code¹³⁾ for a 7.2 MeV neutron. Good agreement is obtained. A small amount of neutrons observed in the light output region more than 4 MeVee may be due to a background from the neutrons and protons generated by the interaction of ${}^{13}\text{C}$ with contamination components in the hydrogen gas, such as air and va-

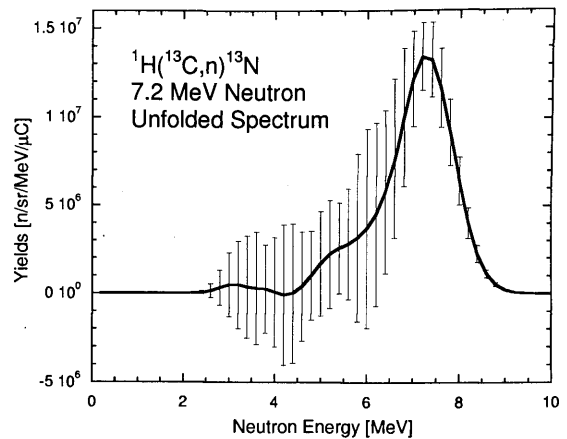


Fig. 8 Neutron spectrum at 0° for the ${}^1\text{H}({}^{13}\text{C},n){}^{13}\text{N}$ reaction at 59.3 MeV, which was obtained using the unfolding code FORIST with the response matrices calculated by the SCINFUL code.

por. The neutron spectrum unfolded with the FORIST code¹⁴⁾ using the response matrices calculated with the SCINFUL code is shown for the measurement at 0° in Fig. 8. The peak energy of 7.2 MeV coincides with the simulation result. The energy resolution was about 1.5 MeV, which is due mainly to the intrinsic resolution of the NE213 scintillator used.

The experimental yields of neutrons produced at 0° are shown together with the calculated ones in Table 1. These experimental errors contain systematic errors of 12.3% and 7%, respectively, for the measurements with the NE213 and ARPRT detectors, in addition to statistical errors. Both the yields measured with the NE213 and ARPRT detectors are in good agreement within the error. It is found that the experimental yields for both neutron energies agree well with the calculated ones with the (p,n) cross sections of Gibbons.⁵⁾ It should be noted that the data of Dagley et al.⁶⁾ was still used for the (p,n) angular distributions because their data is only the available experimental data. As shown in Fig. 3, there are some differences among the measurements. This work may support the smaller cross sections in the energy region of interest.

In Fig. 9, the experimental angular distributions of the neutrons produced by the ${}^1\text{H}({}^{13}\text{C},n)$ and $\text{D}(d,n)$ reactions are plotted together with those calculated using the above-mentioned simulation code. Both the calculated angular distributions are normalized to the experimental values at 0° , respectively. It should be noted that the neutrons

Table 1 Comparison between measured neutron yields at 0° and those calculated with the cross sections of Dagley et al.⁶⁾ and Gibbons.⁵⁾

Incident Energy [MeV]	59.3	56.0
Neutron Energy [MeV]	7.2	6.2
Measured Yields [10^7 n/sr/ μ C]		
NE213	2.42 ± 0.30	1.46 ± 0.18
ARPR	2.05 ± 0.14	1.35 ± 0.09
Calculated Yields [10^7 n/sr/ μ C]		
Dagley et al.	3.71	2.46
Gibbons	2.19	1.53

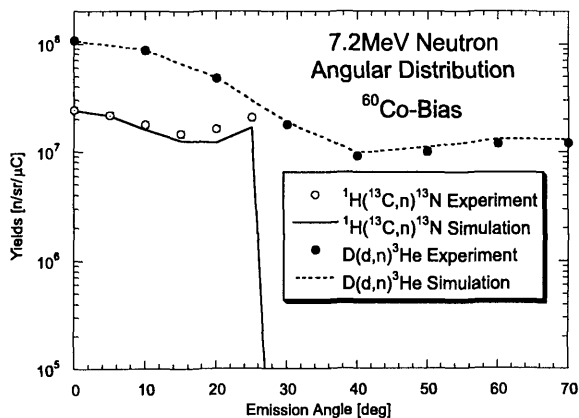


Fig. 9 Angular distributions of neutrons produced by the $^1\text{H}(^{13}\text{C},n)$ and $\text{D}(d,n)$ reaction. The open and closed circles are the experimental data and the solid and dotted lines are the calculated angular distributions.

generated from the $^1\text{H}(^{13}\text{C},n)$ were not observed at angles over 30° . The experimental angular distributions are in good agreement with the calculations for both the reactions. Thus, it was experimentally confirmed that neutrons produced by the $^1\text{H}(^{13}\text{C},n)$ reaction are emitted within the forward cone restricted by the kinematics, whereas neutrons from the $\text{D}(d,n)$ reaction are emitted over the wide angular range.

5. Conclusion and outlook

We have started the R & D of a quasi-monoenergetic neutron source using the $^1\text{H}(^{13}\text{C},n)$ reaction at KUTL. The hydrogen gas target was fabricated as a major apparatus of the neutron source. The feasibility test experiment with 59.3 MeV $^{13}\text{C}^{6+}$ beam has demonstrated that this inverse (p,n) reaction can produce "kinematically collimated" monoenergetic neutrons with 7.2 MeV

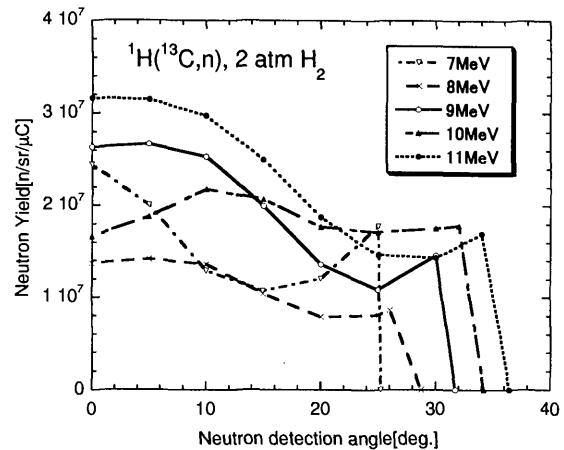


Fig. 10 Estimated angular distributions of neutrons produced by the $^1\text{H}(^{13}\text{C},n)$ reaction using a newly designed gas target.

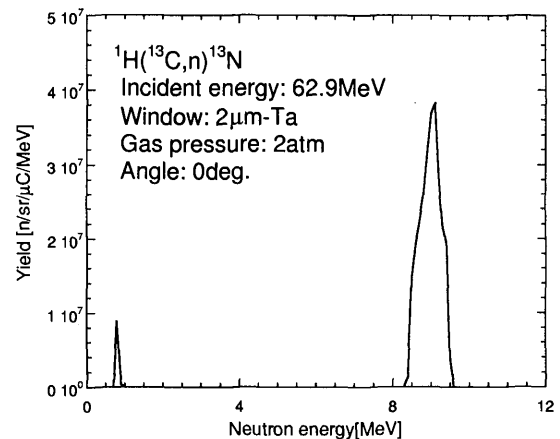


Fig. 11 Estimated spectrum of neutrons produced in the 0° direction by the $^1\text{H}(^{13}\text{C},n)$ reaction at 62.9 MeV using a newly designed gas target.

at 0° .

The present work is the first step toward completion of the monoenergetic $^1\text{H}(^{13}\text{C},n)$ neutron source at KUTL. Further optimization of the design is necessary for enhancement of neutron yields and reduction of backgrounds in order to satisfy several requirements for practical use. For instance, it is desirable that the entrance window of the gas target is as thin as possible in order to reduce the energy loss of the incident ^{13}C beam in it. A simulation of neutron production was carried out for use of $2\ \mu\text{m}$ -thick tantalum foil as the entrance window, which is the thinnest among commercially available tantalum foil. The result with 2 atm hydrogen gas is shown in Figs. 10 and 11. In the simulation, the (p,n) cross sections were

taken from Gibbons.⁵⁾ It was found that use of this new gas-target makes it possible to produce monoenergetic neutrons up to a maximum energy of 11 MeV at KUTL, and all generated neutrons are emitted in the kinematically-allowed forward cone as shown in Fig. 10.

In the future, we plan to carry out systematic measurements of activation cross sections and calibration of neutron detectors using the developed monoenergetic neutron source in the "gas" region between 8 and 14 MeV where the experimental data are scarce.

Acknowledgments

The authors are grateful to Dr. S. Meigo, Japan Atomic Energy Research Institute, for his valuable advice on neutron source simulation and neutron detection. This work was partly supported by a Grant-in-Aid (FY2000) for Encouragement of Young Researchers of the Faculty of Engineering Sciences, Kyushu University, and a Grant-in-Aid for Scientific Research of the Japanese Ministry of Education, Culture, Sports, Science and Technology (No. 13558064).

References

- 1) K. Hasegawa et al., Proc. 11th Int. Conf. Cyclotrons and Their Applications, Tokyo, Japan, October 20-24, 1987, p.642 (1987).
- 2) S. Chiba et al., Nucl. Instr. and Meth., **A281**, 141 (1989).
- 3) M. Drogg, Nucl. Sci. Eng., **106**, 279 (1990).
- 4) Y. Ikeda et al., Proc. of Int. Conf. on Nucl. Data for Sci. and Tech., 13-17 May 1991, Jülich, p.294 (1992).
- 5) J.H. Gibbons et al., Phys. Rev., **114**, 571 (1959).
- 6) P. Dagley et al., Nucl. Phys., **24**, 353 (1961).
- 7) O. Dietzsch, Nucl. Phys., **85**, 689 (1966).
- 8) E. Ramström, Research Report NFL-6, The Studsvik Science Research Laboratory (1979).
- 9) S. Meigo, Japan Atomic Energy Research Institute, JAERI M-94-019, p.243 (1994).
- 10) H. Nishimori et al., Kyushu University Tandem Accelerator Laboratory Report, KUTL-5, p.91 (1995).
- 11) H. Nishimori et al., Nucl. Phys., **A631**, 697c (1998).
- 12) S. Hachiya et al., Kyushu University Tandem Accelerator Laboratory Report, KUTL-7, p.129 (2000); Master thesis (in Japanese), Kyushu University (1999).
- 13) J.K. Dickens, Report ORNL-6452, Oak Ridge National Laboratory (1988).
- 14) R.H. Johnson et al., Nucl. Sci. Eng., **73**, 93 (1980).